Dynamic Relationships among Type IIa Bacteriocins: Temperature Effects on Antimicrobial Activity and on Structure of the C-Terminal Amphipathic α Helix as a Receptor-Binding Region‡

Kamaljit Kaur,§ Lena C. Andrew,|| David S. Wishart,|| and John C. Vederas*,§

Department of Chemistry, University of Alberta, Edmonton, Alberta, Canada, T6G 2G2, and Faculty of Pharmacy and Pharmaceutical Sciences, University of Alberta, Edmonton, Alberta, Canada, T6G 2N8

Received November 11, 2003; Revised Manuscript Received May 12, 2004

ABSTRACT: Dynamic aspects of structural relationships among class IIa bacteriocins, which are antimicrobial peptides from lactic acid bacteria (LAB), have been examined by use of circular dichroism (CD), molecular dynamics (MD) simulations, and activity testing. Pediocin PA-1 is a potent class IIa bacteriocin, which contains a second C-terminal disulfide bond in addition to the highly conserved N-terminal disulfide bond. A mutant of pediocin PA-1, ped[M31Nle], wherein the replacement of methionine by norleucine (Nle) gives enhanced stability toward aerobic oxidation, was synthesized by solid-phase peptide synthesis to study the activity of the peptide in relation to its structure. The secondary structural analysis from CD spectra of ped[M31Nle], carnobacteriocin B2 (cbn B2), and leucocin A (leuA) at different temperatures suggests that the α-helical region of these peptides is important for target recognition and activity. Using molecular modeling and dynamic simulations, complete models of pediocin PA-1, enterocin P, sakacin P, and curvacin A in 2,2,2-trifluoroethanol (TFE) were generated to compare structural relationships among this class of bacteriocins. Their high sequence similarity allows for the use of homology modeling techniques. Starting from homology models based on solution structures of leuA (PDB code 1CW6) and cbnB2 (PDB code 1CW5), results of 2−4 ns MD simulations in TFE and water at 298 and 313 K are reported. The results indicate that these peptides have a common helical C-terminal domain in TFE but a more variable β sheet or coiled N terminus. At elevated temperatures, pediocin PA-1 maintains its overall structure, whereas peptides without the second C-terminal disulfide bond, such as enterocin P, sakacin P, curvacin A, leuA, and cbnB2 experience partial disruption of the helical section. Pediocin PA-1 and ped[M31Nle] were found to be equally active at different temperatures, whereas the other peptides that lack the second C-terminal disulfide bond are 30−50 times less antimicrobially potent at 310 K (37 °C) than at 298 K (25 °C). These results indicate that the structural changes in the helical region observed at elevated temperatures account for the loss of activity of these peptides. The presence of C-terminal hydrophobic residues on one side of the amphipathic helix in class IIa bacteriocins is an important feature for receptor recognition and specificity toward particular organisms. This study assists in the understanding of structure−activity relationships in type IIa bacteriocins and demonstrates the importance of the conserved C-terminal amphipathic α helix for activity.

Fermentation of lactic acid bacteria (LAB)[1] is an age-old method for prolonged safe storage of food. The preservative effect of LAB is partially due to the fermentation of sugar, which results in the production of large amounts of lactic acid (*1*). The resulting low pH environment effectively prevents outgrowth of almost all potential spoilage microorganisms. However, it is clear that LAB combat microorganisms by at least one other mechanism, namely, by secretion of ribosomally synthesized antimicrobial peptides. These peptides, called bacteriocins, seem to be primarily aimed at other LAB, which are likely to be the most prominent competitors in the acidic environment in which these bacteria reside. However, LAB bacteriocins also show potent activity toward a number of potential Gram-positive food spoilage and pathogenic bacteria, e.g., *Listeria*. Generally, the LAB and their bacteriocins display no toxicity toward humans or other eukaryotes. Bacteriocins are already widely used as natural food preservatives and possess great potential in medical applications as alternatives to conventional antibiotics (*2*).

‡ Dedicated to Professor Heinz G. Floss on the occasion of his 70th birthday.

* To whom correspondence should be addressed. Telephone: 780-492-5475. Fax: 780-492-8231. E-mail: john.vederas@ualberta.ca.

§ Department of Chemistry.

|| Faculty of Pharmacy and Pharmaceutical Sciences.

[1] Abbreviations: Acm, acetamidomethyl; Boc, *tert*-butyloxycarbonyl; tBu, *tert*-butyl; cbnB2, carnobacteriocin B2; CD, circular dichroism; curA, curvacin A; DCM, dichloromethane; DMF, *N*,*N*-dimethylformamide; DPC, dodecyl phosphocholine; *e*, electronic charge ($e = 1.602 \times 10^{-19}$ C); entP, enterocin P; Fmoc, 9-fluorenylmethyloxycarbonyl; HPLC, high-performance liquid chromatography; LAB, lactic acid bacteria; leuA, leucocin A; MALDI−TOF, matrix-assisted laser desorption ionization−time-of-flight; MD, molecular dynamics; Nle, norleucine; NMP, *N*-methylpyrrolidinone; OD, optical density; pedPA-1, pediocin PA-1; PTS, phosphotransferase system; RMSD, root-mean-square deviation; sakP, sakacin P; SEM, standard error (of the mean); SPC, single point charge; TFA, trifluoroacetic acid; TFE, 2,2,2-trifluoroethanol; Trt, trityl.

10.1021/bi036018e CCC: $27.50
Published on Web 06/25/2004

Table 1: Amino Acid Sequences of Some Class IIa Bacteriocins[a]

Bacteriocin	Amino acid Sequence	Ref.
Pediocin PA-1	KY**YGNGV**TCG KHSCSVDWGK ATTCIINNGA MAWATGGHQG NHKC	(*23*)
Enterocin P	ATRS**YGNGV**YCN NSKCWVNWGE AKENIAGIVI SGWASGLAGM GH	(*24*)
Sakacin P	KY**YGNGV**HCG KHSCTVDWGT AIGNIGNNAA ANWATGGNAG WNK	(*25*)
Mesentericin Y105	KY**YGNGV**HCT KSGCSVNWGE AASAGIHRLA NGGNGFW	(*16*)
Leucocin A	KY**YGNGV**HCT KSGCSVNWGE AFSAGVHRLA NGGNGFW	(*5*)
Carnobacteriocin B2	VN**YGNGV**SCS KTKCSVNWGQ AFQERYTAGI NSFVSGVASG AGSIGRRP	(*26*)
Curvacin A	ARS**YGNGV**YCN NKKCWVNRGE ATQSIIGGMI SGWASGLAGM	(*27*)

[a] YGNGV motif (bold) and residues in the C-terminal domain forming the amphipathic α helix (red) are highlighted.

An important group of these antimicrobial peptides are the pediocin-like, class IIa bacteriocins produced by LAB (*3*, *4*). We reported the purification and primary structure of the first of this class, leucocin A (leuA) (*5*), but in the meantime, over 20 such peptides have been identified. These heat-stable, cationic peptides typically have 37−48 amino acid residues and display potent antilisterial activity. Class IIa bacteriocins contain at least one conserved disulfide bond, a highly conserved N-terminal YGNGV sequence, and a variable hydrophobic C-terminal domain (Table 1). They are believed to exert their antibiotic activity by forming pores in the cell membrane of sensitive bacteria (*6*, *7*). They show high levels of specificity for a particular target organisms among closely related groups. Although many interesting aspects of these peptides have been investigated (*4*, *8*−*10*), including regulation of production, target-cell sensitivity, immunity, and resistance, the exact details of interaction with the target cell at the molecular level are still unknown.

Class IIa bacteriocins are essentially unstructured in water but become partly structured in the presence of 2,2,2-trifluoroethanol (TFE) or membrane-mimicking environments such as detergent micelles or vesicles (*11*−*16*). TFE has become a common solvent for structure elucidation of hydrophobic peptides, especially ones that act on membrane-bound protein receptors. Although the mechanism by which TFE induces defined conformations in small peptides is not completely understood, a number of studies suggest that the stabilizing effect of TFE is due to the preferential aggregation of TFE molecules around the peptide, providing a low dielectric constant and hydrophobic environment (*17*−*19*). Structural studies including the NMR solution structure of leuA (*11*), carnobacteriocin B2 (cbnB2) (*13*), and sakacin P (sakP) (*20*) and circular dichroism (CD) structural studies of pediocin PA-1 (pedPA-1) (*14*) in TFE or membrane-mimicking conditions (e.g., dodecyl phosphocholine (DPC) micelles) show the presence of one common structural feature in these peptides, namely, 30−45% α-helical content. The Edmundson helical wheel analysis (*21*) of most of these peptides indicates that they form amphipathic α helix in the C-terminal domain. The exact function of this helical domain, which is important for recognition and/or activity, is not yet clear. However, replacement of a hydrophobic residue Phe33 with a polar Ser in the α-helical region of cbnB2 completely abolished antimicrobial activity and drastically altered its retention time on reverse-phase HPLC (*22*). In contrast, substitution of certain polar residues in the C terminus beyond the helical region (e.g., Arg46 to Gly) had little or no effect (*22*). Similarly, replacement of Trp33 within the α helix in sakP with the hydrophobic residues Leu or Phe had marginal effects on activity, whereas replacement with the more polar Arg reduced activity 500−1000 times (*28*). Thus, the hydrophobic residues in the amphipathic α-helical region can only be substituted with another hydrophobic residue and not with any polar residue. However, beyond the helical region, some replacement of residues with polar or hydrophobic amino acids can be tolerated. This indicates that maintaining the hydrophobicity of the amphipathic helix is critical for activity.

Many studies have focused on identifying the domains and amino acid residues responsible for activity in these peptides (*28*−*32*). However, only a few have been aimed at identifying the location and kind of interaction with the target cell of this class of bacteriocins (*33*−*35*). Class IIa bacteriocins mainly display a narrow and strain-specific spectrum of activity. The minor differences in phospholipid composition between strains of the same species or between related species cannot explain such a highly specific spectrum of activity. An enantiomer of leuA, in which all amino acids have D configuration, was found to be completely lacking in antimicrobial activity, thereby demonstrating that a chiral interaction is required at the target-cell surface for the bacteriocin to display its effects (*36*). As discussed in that report (*36*), synthetic D enantiomers of natural peptides (e.g., mellitin and magainin) that do not require chiral interaction with a receptor molecule and work directly by membrane disruption will display full biological activity. This is not the case with the type IIa bacteriocin leuA. This points toward the involvement of a receptor protein as a target molecule in sensitive bacterial cells. Recently, a mannose phosphotransferase system (PTS) permease (EII_t^{Man}) has been proposed to be a target molecule for mesentericin Y105 and leuA (*33*−*35*). Hechard et al. (*34*, *35*) proposed EII_t^{Man} to be the target receptor for all class IIa bacteriocins in *Listeria monocytogenes*, *Enterococcus faecalis*, and other sensitive bacteria. An additional extracellular domain present in the MptD subunit of EII_t^{Man} compared to other mannose PTS EII sequences is suggested to be involved in class IIa bacteriocin sensitivity. An in-frame deletion of this section of *mptD* led to resistance of *L. monocytogenes* to mesentericin Y105, showing its connection with sensitivity to this peptide (*35*).

pedPA-1 is a very active class IIa bacteriocin with an additional C-terminal disulfide bond that makes its structure particularly interesting. In the present study, we chemically synthesize a mutant of pedPA-1, ped[M31Nle], wherein the replacement of methionine by norleucine (Nle) gives enhanced stability toward aerobic oxidation. We then examine the structure and activity of the mutant, as well as the parent pedPA-1 and compare it to related bacteriocins without the C-terminal disulfide bond such as leuA, cbnB2, enterocin P (entP), sakP, and curvacin A (curA) using CD and molecular dynamics (MD) simulations at different temperatures. The antimicrobial activities of pedPA-1, ped[M31Nle], leuA, and cbnB2 were monitored as a function of the temperature against two strains, *Listeria innocua* ATCC 33091 and *Carnobacteriocin divergens* LV13. Homology-modeled structures of additional representative type IIa bacteriocins, pedPA-1, entP, sakP, and curA were generated, and their behavior in TFE and water was monitored using MD simulation at 298 and 313 K. The secondary structural information obtained from the CD data analysis correlates to the temperature effects and relationships obtained from the antibiotic activity studies and the MD simulations. The results confirm the importance of maintaining the structural

integrity of the α-helical region for optimal activity and molecular recognition by the target receptor.

MATERIALS AND METHODS

Pediocin (M31Nle) Synthesis, Purification, and Characterization. Stepwise synthesis of synthetic pediocin (*syn*-pediocin) with a point mutation at residue 31 (Met31Nle) was done manually on a 0.3-mmol scale of Wang resin (1.0% DVB cross-linked) following the standard Fmoc solid-phase peptide chemistry as described previously (*36*). Fmoc-protected L-amino acids were used, and the following side-chain protection was used Asn(Trt), Asp(tBu), Cys(Acm), Cys(Trt), Glu(tBu), His(Trt), Lys(Boc), Ser(tBu), Thr(tBu), Trp(Boc), and Tyr(tBu). The four cysteine residues that form two disulfide bonds were orthogonally protected [residues 9 and 14 Cys(Acm) and residues 24 and 44 Cys(Trt)]. From residue 15 onward, *N*-methylpyrrolidinone (NMP) was used as a solvent in place of DMF during deprotection and coupling steps (*37*). To facilitate the coupling of difficult residues (Asn, Ile, and most of the residues after position 15) elevated temperatures of up to 50 °C (*37*, *38*) and magic mixture (*37*, *38*) solvents were employed. A test cleavage was performed after each five residues were coupled, and the desired product was confirmed by MALDI−TOF mass spectrometry. Each test peptide was cleaved from the resin with a mixture of 87.5% TFA, 5% phenol, 5% water, 2.5% dithiothreitol, and 2.5% anisole for 90 min at room temperature with mechanical shaking.

The completed peptide resin was stored at −20 °C under argon, with the N-terminal Fmoc group still attached. Prior to all oxidative transformations and/or acid cleavages or deprotections, N-terminal Fmoc was removed by treatment with piperidine−NMP (4 × 5 mL, 5 min), followed by washes with DMF and 2-propanol. The peptide chain was released from support, with concomitant removal of acid-labile side-chain protecting groups using the same procedure as used for the test cleavages. The filtrate from the cleavage reactions was collected, combined with TFA washes (3 × 2 min, 1 mL), and concentrated in vacuo. Cold diethyl ether (∼15 mL) was added to precipitate the crude cleaved peptide. After trituration for 2 min, the peptide was collected upon centrifugation and decantation of the ether. The crude peptide precipitate dissolved in 40% MeCN was purified on a preparative Zorbax RX-C8 HPLC column (21 × 250 mm, flow rate = 8 mL/min, monitored at 220 nm) using a gradient of 10−40% MeCN in 0.05% aqueous TFA over a period of 1 h. The fractions showing the desired mass of 4751.3 [MH^+, reduced peptide with 2 Cys(Acm)] were collected and lyophilized. The dried fractions were dissolved in TFE/water (1:1, v/v), buffered to pH 7.6 with ammonium bicarbonate, and stirred overnight under O_2 at room temperature. At this stage, the reaction mixture was acidified with HCl (1 M) and vacuum-evaporated followed by dissolution in acetic acid/water (4:1, v/v). Removal of Acm groups along with the disulfide-bond formation was achieved by stirring the reaction mixture with I_2 (0.1 M in methonal) under argon for 2 h. The oxidation was quenched by the addition of aqueous ascorbic acid (1 M), and the crude product was purified by reverse-phase HPLC. The fractions were collected and lyophilized to give a yield of 18 mg of pure synthetic pediocin (M31Nle) (calculated overall yield of 3.8%). Purity was confirmed by HPLC and MALDI−TOF mass spectrometry (4607.3, MH^+).

Production, Isolation, and Purification of pedPA-1. The fermentation of *Pediococcus acidilactici* PAC 1.0 was done as reported previously (*14*) with some modifications in the isolation and purification procedures. Isolation and purification was done by a rapid three-step procedure. The cells were removed from 14-h cultures by centrifugation, and the supernatant was loaded directly onto an Amberlite XAD-16 (BDH Chemicals) column (2.5 × 12 cm) preequilibrated with milliQ water and sequentially washed with 30% ethanol and 70% 2-propanol (pH 2.0) at a flow rate of 15 mL/min. The most active fraction (70% 2-propanol) was concentrated in vacuo at 30 °C to 15 mL. It was then applied onto a C18 MegaBond Flash Column (Varain) preequilibrated with milliQ water and sequentially washed with water (50 mL), 30% EtOH (50 mL), 20% 2-propanol (40 mL), 40% 2-propanol (40 mL), and finally 70% 2-propanol at pH 2.0 (100 mL). The most active fraction (70% 2-propanol) was concentrated to 1 mL and was further purified by HPLC as described by Watson et al. (*14*). From a culture media of 3 L, about 1 mg of pure pedPA-1 was obtained (4625, MH^+).

Antimicrobial Activity. Bacteriocin activity was measured using an assay system essentially as described by Fimland et al. (*28*). Tubes containing culture medium (2 mL), with bacteriocin (pedPA-1, ped[M31Nle], leuA, or cbnB2) fractions at 2-fold dilutions and the indicator strains *L. innocua* ATCC 33091 and *C. divergens* LV13 at an OD_{590} of about 0.01, were incubated at 25 and 37 °C. After 14−16 h, the culture media (200 μL) was transferred into wells of a microtiter plate and growth of indicator strain was measured spectrophotometrically at 590 nm with a microtiter plate reader (Thermomax, Molecular Devices). The minimal inhibitory concentration (MIC) was defined as the concentration of bacteriocin that inhibited the growth of the indicator strain by 50%. Each sample was done three times, and the experiments were repeated at least twice. leuA and cbnB2, prepared in our laboratory previously (*11*, *13*), were purified using analytical HPLC prior to use. Their purity was further confirmed by MALDI−TOF mass spectrometry. The concentration of bacteriocins was determined by measuring UV absorption at 280 nm, which was converted to protein concentration using molecular extinction coefficients. The molecular extinction coefficients were calculated from the contribution of individual amino acid residues. Class IIa bacteriocins are unstructured in water (*11*, *14*), and it has been previously shown that the UV method is fairly reliable for concentration determination (*39*).

CD Spectroscopy. All CD measurements were made on a Jasco J-720 spectrophotometer in a thermally controlled quartz cell with a 0.02-cm path length over 190−250 nm. For the first set of experiments, CD spectra of pedPA-1 and ped[M31Nle] in 0 and 90% TFE in 0.1% aqueous TFA (pH ∼2.0) at 25 °C were collected. The concentrations of pedPA-1 and ped[M31Nle] used were 40 and 35 μM, respectively. The second set of experiments was performed using ped[M31Nle], leuA, and cbnB2 in 90% TFE (0.1% aqueous TFA) at 25 and 37 °C. The final concentrations of the peptides were obtained by amino acid analysis. Data were collected every 0.05 nm and were the average of 8 scans. The bandwidth was set at 1.0 nm and the sensitivity, at 50 mdeg. The response time was 0.25 s. In all cases, baseline

scans of aqueous buffer were subtracted from the experimental readings. Results were expressed in units of molar ellipticity per residue (deg cm^2 $dmol^{-1}$) and plotted versus the wavelength. Analysis of the CD spectra involved quantitative curve fitting using the CDPro software analysis program (*40*). This software uses three programs to perform the protein secondary structure analysis from CD spectra. An input file for all three programs is created using CRDATA (provided in CDPro), which converts molar ellipticity values into molar CD per residue [$\Delta\epsilon$/n]. A set of 48 reference proteins from 5 different sources is used in this software package. The three CD analysis programs CONTIN/LL, SELCON3, and CDSSTR use a different algorithm for analyzing a given protein CD spectrum. Output data for each of the three programs were given in terms of fractions of six different secondary structure classes, namely, regular α helix, distorted α helix, regular β strand, distorted β strand, turns, and unordered. Because the same set of reference proteins was used by each of the three programs, their fractional secondary structures could be averaged. For convenience of data interpretation, the regular and distorted components of α helix and β strand and turns and unordered structural elements were added to give overall helical, strand, and coil structures, respectively. The final secondary structure elements were the average from the triplicate samples for each peptide, and the standard error was calculated for each of them. Each was also examined separately using the three analysis programs mentioned above, and the standard error was calculated for each of them. The latter results are all within the experimental error given.

Modeling and Simulation Methods. The sequences corresponding to pedPA-1, entP, sakP, and curA were searched against the SWISSPROT (*41*) and Protein Data Bank (*42*) databases using both FASTA (*43*) and BLAST (*44*). All bacteriocins showed high sequence identity with leuA (PDB code 1CW6) or cbnB2 (PDB code 1CW5) for which the three-dimensional NMR structure in TFE has been determined previously (*11*, *13*). Multiple amino acid sequence alignments and initial homology-based structures were done using the "magic fit" module of Swiss-PdbViewer 3.7 (*45*). These homology-based structures were chosen as the starting structures for subsequent MD simulations. MD simulations of solvated bacteriocins in TFE or water were performed using a parallel version of the GROMACS 3.1 MD simulation package (GROMOS96 force field) (*46*) on a dual Pentium III personal computer processor machine running LAM-MPI version 6.5.4 (*47*). The parallelized MD code reduced the computational time by approximately 50% compared to the serial version of GROMACS. TFE solvent was parametrized according to Fioroni et al. (*48*), which attributes the following charges to the TFE atoms: F = −0.17*e*, C = 0.452*e*, CH2 = 0.273*e*, OA = −0.625*e*, and HO = 0.410*e* (where OA and HO are the hydroxylic oxygen and hydrogen atoms, respectively, for the GROMOS force field). Water molecules were represented by means of the SPC model, which attributes a charge of 0.41*e* and −0.82*e* to the hydrogen and oxygen atoms, respectively (*49*).

All systems were simulated in the NPT ensemble at 298 or 313 K using periodic boundary conditions. Weak coupling of the protein to a solvent bath of constant temperature was maintained using the Berendsen thermostat (*50*) with a coupling constant of $\tau_T = 0.1$ ps. The pressure was controlled using the Berendsen algorithm at 1 bar with a coupling constant $\tau_P = 4$ ps, using a compressibility of liquid TFE of 1.22×10^{-4} and 1.34×10^{-4} kJ^{-1} mol nm^3 at 298 and 313 K, respectively (*48*). For simulations in water, τ_P was 0.5 ps and a compressibility of 4.5×10^{-5} kJ^{-1} mol nm^3 was used. The electrostatic and van der Waals interactions were truncated at a cutoff distance of 1.2 nm. The integration time step was 2 fs, and the coordinates and velocities were saved every 2 ps. The LINCS algorithm was used to restrain all bond lengths (*51*).

All bacteriocins were considered to have positively and negatively charged N-terminal NH_3^+ and C-terminal COO^- groups, respectively. Asp, Lys, Arg, and Glu residues were considered to be charged, whereas His residues were kept neutral. pedPA-1, entP, sakP, and curA had a total final charge of +3*e*, +1*e*, +2*e*, and +3*e*, respectively. Preliminary calculations were also done with pedPA-1 in a fully protonated state (pH ∼2), and no significant structural differences were observed from the charge arrangement described above (data not shown). Simulation systems were generated by peptide insertion into a cubic box with an edge length of ca. 6 nm, followed by solvation of the protein using TFE or SPC water molecules. The system was initially subjected to 1000 steps of the steepest descent energy minimization. The protein coordinates of the resulting systems were then restrained, while allowing solvent molecules to relax their positions and optimize interactions with the protein during a 200-ps simulation. After initial equilibration, 2−4 ns MD simulations were run. The peptides in TFE and water showed a stationary behavior of the potential energy after about 200 ps. Snapshots of the peptide structures extracted from the last 1 ns of the MD simulation were averaged and minimized further using a conjugate gradient algorithm. Simulations were analyzed using GROMACS routines. Secondary structures were analyzed using VADAR (*52*). SwissPDB Viewer (*45*) and WebLab ViewerLite (*53*) were used to visualize and superimpose the structures.

RESULTS

Synthetic Pediocin (M31Nle). ped[M31Nle] was synthesized with a mutation at Met31, the single methionine residue in pedPA-1. This residue is prone to oxidation, and oxidized pediocin has been shown to be 100 times less antimicrobially active than the unoxidized form toward most of the indicator strains (*29*). Thus, this stable mutant was made to allow accurate activity and structural studies on this bacteriocin. ped[M31Nle] was synthesized using Fmoc/tBu chemistry with orthogonal protection of four cysteine residues to facilitate proper disulfide-bond formation. The proper folding of the C-terminal disulfide bond (between residues 24 and 44) was achieved by oxidizing it in buffered TFE/H_2O (pH 7.6) under an O_2 environment. NMR studies have shown that these peptides adopt a well-defined tertiary structure in solvents such as TFE and DPC micelles (*11*, *13*). Iodine was used as the oxidizing agent to form the short N-terminal disulfide bond (between residues 9 and 14). A total of 18 mg of pure ped[M31Nle] was obtained for activity and structural studies.

Comparisons of Antimicrobial Activity. The activity spectra of pedPA-1 and ped[M31Nle] were found to be quite similar. Replacing Met by Nle protected the peptide from oxidation,

Table 2: Activity of Class IIa Bacteriocins as a Function of Temperature[a]

	MIC (nM) ± SEM[b]			
	L. innocua		*C. divergens*	
	25 °C	37 °C	25 °C	37 °C
pedPA-1	1.4 ± 0.3	5.3 ± 0.4	3.3 ± 0.2	29.5 ± 0.7
ped[M31Nle]	2.7 ± 0.6	7.7 ± 0.9	4.6 ± 0.8	20.9 ± 1
leuA	1.1 ± 0.4	35.0 ± 1	1.0 ± 0.3	33.5 ± 0.9
cbnB2	7.4 ± 0.6	334 ± 10	8.7 ± 0.5	450 ± 20

[a] Bacteriocin activity was measured as described under the Materials and Methods. The indicator strains used in the bacteriocin assay were *L. innocua* ATCC 33091 and *C. divergens* LV13. [b] MIC is the concentration of bacteriocin that inhibited growth of the indicator strain by 50%. The values are results of at least three independent measurements.

which reduces the activity of pedPA-1 with time, and had only very minor effects on initial bacteriocin activity. Both the peptides were found to be almost equally potent against indicator strains *L. innocua* and *C. divergens* (Table 2). Previously, Johnsen et al. have shown that replacing Met by Ala, Ile, or Leu at position 31 of pedPA-1 by site-directed mutagenesis did not alter the activity spectrum of this peptide for most indicator strains (*32*). When assayed at 25 and 37 °C, pedPA-1 and ped[M31Nle] had nearly the same potency (3−4 times less activity) at two temperatures with the exception of pedPA-1 against *C. divergens* (9 times less active). The loss in activity of pedPA-1 at higher temperatures is almost certainly due to more rapid oxidation of Met at elevated temperatures to generate the much less-active methionine-sulfoxide-containing derivative. Johnsen et al. have shown that during storage conditions pedPA-1 changes to a less-active form (100-fold less active) with an increase in the molecular mass by 16 Da (*32*). leuA and cbnB2, which lack the C-terminal disulfide bond and do not have methionine residues, lost their activity up to 30−50 times at higher temperatures (Table 2).

CD Spectroscopy. CD spectroscopy was used to compare the structures of native pedPA-1 and ped[M31Nle]. As mentioned above, the formation of the C-terminal disulfide bond in ped[M31Nle] was achieved in TFE/water conditions. This was done to assist the formation of this bond with the correct folding and thereby to maintain its structure as close as possible to native pedPA-1. Spectra for both the peptides were collected in water and 90% TFE containing 0.1% TFA (pH 2.5). In water, these peptides were significantly unstructured, but at a high TFE percentage (90%), the helical structure was induced. This concentration of TFE has been shown previously to induce the maximum structure in this class of bacteriocins (*11*, *14*). Quantitative analysis of the distribution of secondary structure showed that in 90% TFE both peptides were equally structured (Table 3) with 32−35% helix in each of them. ped[M31Nle] was used for further CD experiments at different temperatures because of its stability toward oxidation. Spectra for ped[M31Nle], leuA, and cbnB2 were collected in 90% TFE at 25 and 37 °C. In all three peptides, significant helical structure was induced as indicated by the appearance of distinct negative bands at 206−209 nm, negative shoulders near 220 nm, and positive bands at 195 nm (Figure 1). Spectra at 25 and 37 °C appeared quite similar on initial inspection. This is because there is partial, but not complete, loss of α-helix structure. However,

Table 3: CD Analysis of the Secondary Structure Fractions of Native pedPA-1 and Synthetic ped[M31Nle] in TFE and Water at 25 °C

bacteriocin	solvent[a]	α helix	β sheet	coil
pedPA-1	aqueous	0.08	0.23	0.69
	90% TFE	0.35	0.15	0.50
ped[M31Nle]	aqueous	0.06	0.38	0.57
	90% TFE	0.32	0.19	0.50

[a] All samples were acidified to pH ~2.5 by addition of TFA (0.1% final concentration).

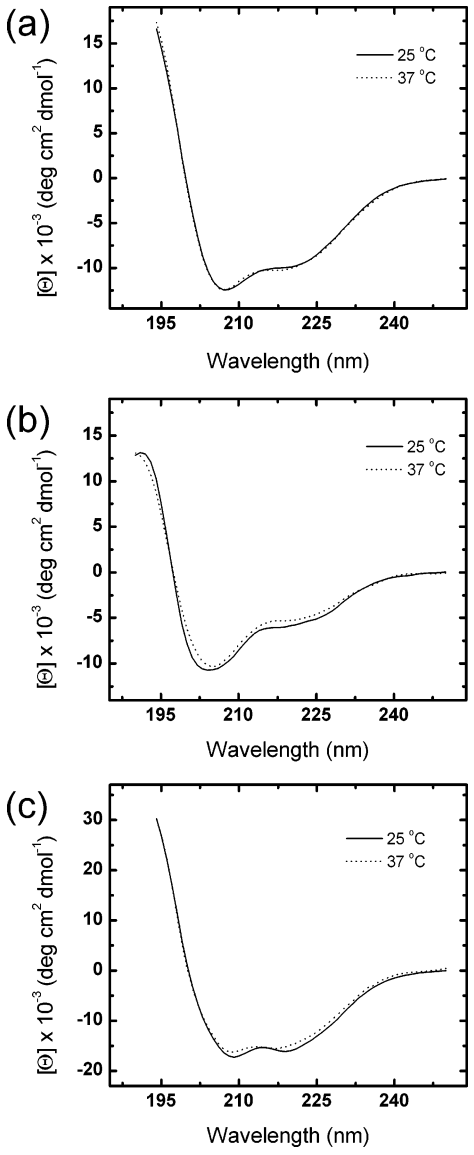

FIGURE 1: CD spectra in 90% TFE (0.1% TFA final concentration, pH 2.5) at 25 °C (—) and 37 °C (····) of (a) ped[M31Nle], (b) leuA, and (c) cbnB2. The ellipticity was expressed as the mean residue molar ellipticity (Θ) in deg cm^2 dmol^{-1}. The secondary structure composition was estimated by deconvolution, as implemented by the CDPro software (*40*).

quantitative analysis of the secondary structure distribution consistently showed a slight but significant decrease in the helical content for leuA and cbnB2 at higher temperatures, whereas the structure of ped[M31Nle] remained essentially the same (Table 4). On the basis of the mean values and the standard error estimates, it is apparent that the secondary structure elements are different for leuA and cbnB2 at two temperatures. Thus, in contrast to the peptides, such as leuA

Table 4: Effect of Temperature on the Secondary Structure Elements Determined by CD Analysis of Various Class IIa Bacteriocins in TFE

bacteriocin[a]	temperature (°C)[b]	α helix[c] ± SEM	β sheet[c] ± SEM	coil[c] ± SEM
ped[M31Nle]	25	0.329 ± 0.006	0.180 ± 0.006	0.490 ± 0.009
	37	0.325 ± 0.005	0.188 ± 0.007	0.483 ± 0.008
leuA	25	0.320 ± 0.005	0.171 ± 0.003	0.508 ± 0.004
	37	0.226 ± 0.009	0.249 ± 0.004	0.520 ± 0.009
cbnB2	25	0.443 ± 0.008	0.117 ± 0.007	0.44 ± 0.01
	37	0.379 ± 0.007	0.15 ± 0.01	0.47 ± 0.01

[a] All samples were prepared three times in TFE/H_2O (9:1, v/v) containing 0.1% TFA (pH ~2.5). [b] Samples were allowed to equilibrate for at least 10 min at a particular temperature before taking CD scans. [c] Secondary structure determination from CD data was done using CDPro software (*40*) as described in the Materials and Methods.

Table 5: Bacteriocins Simulations

bacteriocin	template	sequence identity[a]	total number of solvent molecules[b]	duration (ns)	final Cα RMSD, all residues (nm)[c]
pedPA-1	leuA (1CW6)	15:21 (71%)	1509 TFE	4	0.30
			6926 H_2O	4	0.92
entP	cbnB2 (1CW5)	13:19 (68%)	1502 TFE	4	0.25
sakP	leuA (1CW6)	15:21 (71%)	1514 TFE	4	0.25
			6948 H_2O	4	0.62
curA	cbnB2 (1CW5)	13:21 (62%)	1509 TFE	4	0.24
			6943 H_2O	3	1.31

[a] Most of the sequence identity was present in the N-terminal region. Overall sequence identity was between 32 and 35% for these peptides. [b] Solvent molecules present in a cubic box at a volume of 216 nm^3. [c] For all Cα atoms of the bacteriocin averaged over the last 1 ns of simulation.

and cbnB2, that lack the C-terminal disulfide bond, the presence of the additional C-terminal disulfide bond in ped-[M31Nle] helps maintain the integrity of the helical structure at elevated temperatures.

Homology Modeling. Multiple sequence alignment of class IIa bacteriocins shows that there is about a 60−80% sequence identity in the N-terminal region and a 30−40% overall sequence identity among these peptides. The high sequence identity of pedPA-1, entP, sakP, and curA to leuA and cbnB2, for which the solution structure is known, allows for the use of homology-based techniques for this class of peptides (Table 5). Although the NMR solution structure of sakP became available very recently (*20*), we have used the homology-based structure of sakP for MD studies. A comparison of these structures shows that the modeled structure and NMR structure of sakP in TFE are in good agreement. sakP forms a β-sheet-like structure in the N terminus (residues 1−17) and an amphipathic α-helical structure in the central region toward the C terminus (residues 18−34). Residues 34 to the C-terminal form a coil-like structure that folds back on the helical region. All bacteriocin models were generated in two stages: (i) modeling the structure by fitting to the template (ii) creating the C-terminal disulfide bond (in the case of pedPA-1) by bringing the C-terminal residue (Cys44) close to the Cys24 using different loop structures available in the Swiss Model loop database. The loop structure that allowed the formation of the disulfide bond with minimum perturbation of the C-terminal helix was chosen for energy minimization and subsequent MD simulations.

MD Simulation. MD simulations of pedPA-1, entP, sakP, and curA were done using TFE as a solvent. A recently reported TFE model by Fioroni et al. for condensed phase simulations was used (*48*). The parametrization of this model is based on GROMOS96 force field with the methylene group treated as a united atom. Multi-nanosecond MD simulations were performed on these peptides placed in the center of a cubic box fully solvated with TFE molecules (Table 5). A box with the volume of 216 nm^3 per peptide was chosen to keep the concentration as close as possible to the experimental samples (~5 mM as used for NMR solution structure elucidation). MD simulations were also performed in an aqueous environment for these peptides. In these simulations, the peptide was placed in a cubic box with the volume of 216 nm^3 and was solvated with SPC water molecules (*49*). Table 5 lists the number of TFE or water molecules present per peptide in the cubic box.

A measure of the overall peptide stability was obtained by plotting the root-mean-square deviation (RMSD) of the peptide structure fitted onto its initial structure as a function of time (Figure 2a). Peptides, in general, were stabilized after 1−2 ns in TFE without much further drift. Figure 2b shows RMSD values for pedPA-1, sakP, curA, and cbnB2 in TFE at 313 K. The initial structure used in this case to calculate RMSD was the final MD structure from the 4 ns of simulation for pedPA-1, sakP, and curA and the NMR structure for cbnB2. The RMSD values suggest that raising the temperature did not alter the structure substantially from its initial conformation. However, simulations in water typically destabilized these peptides (see below). Table 5 lists the final RMSD for all Cα atoms of the bacteriocin, averaged over the last 1 ns of the simulations in water and TFE. It is evident from the RMSD values that in each case the peptide remained closer to its starting conformation in TFE than in water.

Figure 3 shows the structures of pedPA-1 in TFE and water at 298 K. Figure 4 shows the structures of entP, sakP, and curA in TFE at 298 and 313 K. Details of the helical structures of pediocin and curvacin are shown in Figure 5. Finally, in Figure 6, we compare the structures of cbnB2 in TFE at 298 and 313 K. Figure 3a and parts a, c, and e of Figure 4 show an energy-minimized average of the configurations taken every 50 ps from a 1 ns of simulation trajectory at the end of the simulation for pedPA-1, entP, sakP, and curA, respectively, at 298 K. In all peptides, some increase in the overall helical content was observed as compared to

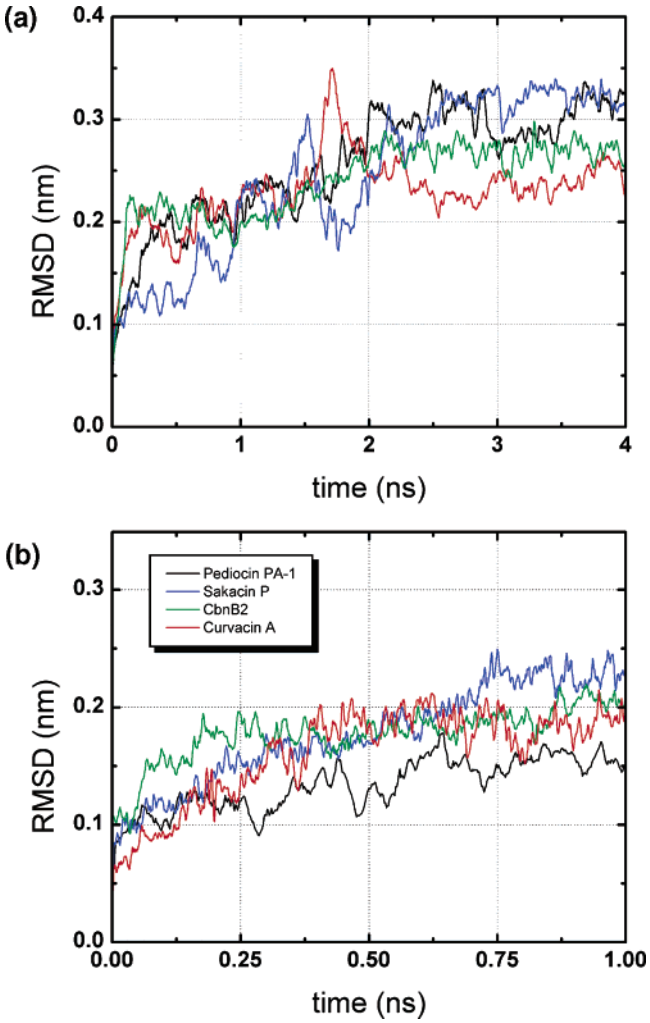

FIGURE 2: (a) Cα RMSD with respect to the minimized initial structure of pedPA-1 (black), entP (green), sakP (blue), and curA (red). These simulations were performed at 298 K. (b) Cα RMSD with respect to the final MD structure from the 4 ns of simulation of pedPA-1, sakP, and curA and NMR solution structure of cbnB2 (green). These simulations were performed at 313 K.

the starting structure. Although TFE was found to be uniformly present around the peptide throughout the trajectory, the interactions between the peptide and TFE did not seem to displace interactions within the peptide. The simulation shows that the peptides maintain a well-defined structure with an α helix toward the C-terminal region and a β sheet or random coil in the N-terminal region throughout the trajectory. A closer look at the α helices (Figure 5) shows that all of them form the amphipathic helix with hydrophobic residues facing out and hydrophilic residues facing in toward the N-terminal β sheet or the coil. Upon increasing the temperature of the system from 298 to 313 K, the structure of pedPA-1 remained intact while, the C-terminal amphipathic helix region of other peptides, namely, entP, sakP, curA, and cbnB2 started uncoiling as shown in parts b, d, and f of Figure 4 and Figure 6b, respectively. The comparison of the secondary structure of various class IIa bacteriocins in TFE at two temperatures, 298 and 313 K, is shown in Table 6.

MD simulation of these peptides in water showed that water had a destructive effect on their structures. Raising the temperature from 298 to 313 K for 1 ns removed all of the secondary structural features from the peptides and

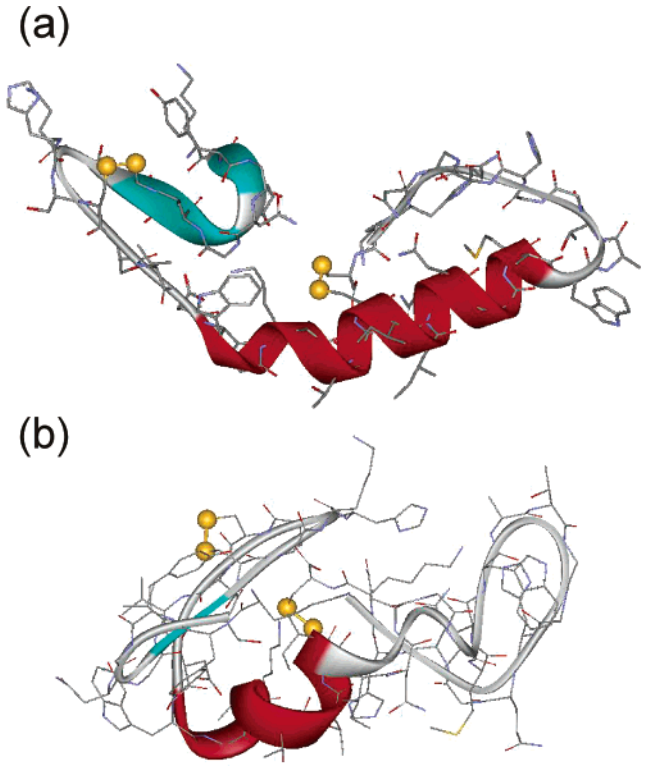

FIGURE 3: Minimized average structure over the last 1 ns of simulation at 298 K for pedPA-1 in (a) TFE and (b) water.

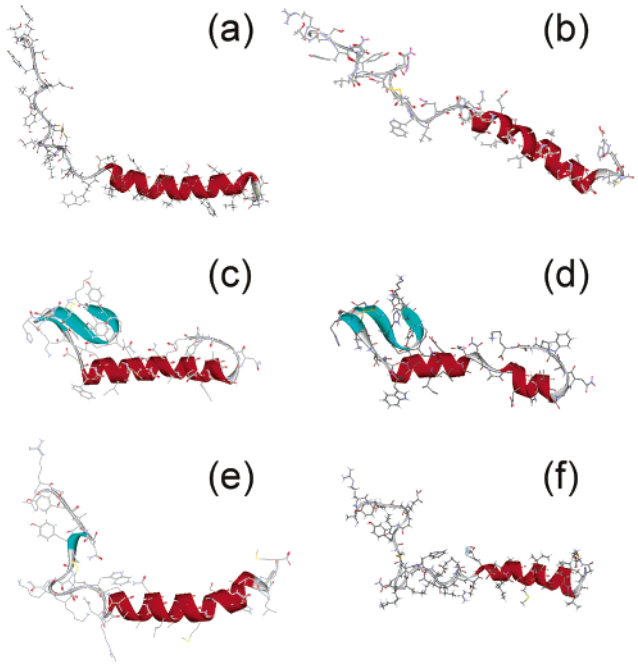

FIGURE 4: Minimized average structure over the last 1 ns of simulation in TFE for entP at (a) 298 and (b) 313 K, sakP at (c) 298 and (d) 313 K, and curA at (e) 298 and (f) 313 K.

rendered them globular. Cooling them back to 298 K for 1 ns did not rescue the secondary structure, suggesting their lack of being structured in water. However, peptides in TFE returned to their original structure upon cooling (not shown here). Simulations in water were typically run for 2 ns at 298 K, followed by 1 ns at 313 K, and finally 1 ns at 298 K. An average of the snapshots from the last 1-ns trajectory was further minimized to get the final structure. Structures of sakP and curA shown in the Supporting Information

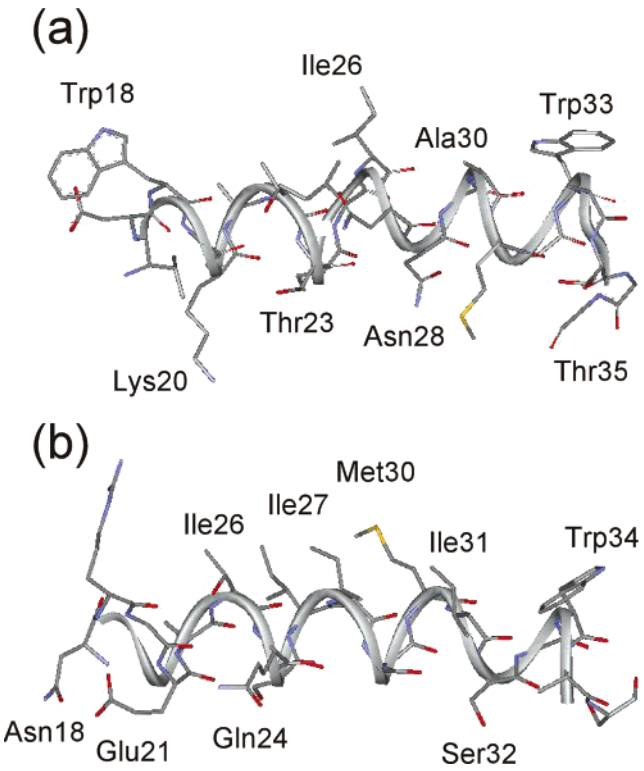

FIGURE 5: Amphipathic helical section of (a) pedPA-1 and (b) curA, highlighting some of the residues.

display similar behavior as pedPA-1 in water (Figure 3b).

DISCUSSION

Antimicrobial peptides (bacteriocins) from LAB disrupt membranes of target bacteria and lead to leakage of cellular contents (*30*, *54*). It is becoming increasingly evident that class IIa bacteriocins act on the target organism by receptor-mediated recognition (*55*), whereby these antimicrobial peptides interact with a putative receptor protein in the membrane of the target cell, with possible subsequent pore formation. Alternative hypotheses have been proposed for the importance of different parts of these peptides. On the basis of the amino acid sequence, the N-terminal region of these peptides is conserved, whereas the C-terminal region is highly variable. In contrast, NMR structural studies of leuA, cbnB2, and sakP in TFE show that the C-terminal region is structurally conserved as an α helix, whereas the N-terminal region is structurally more variable because of the effect of a few key amino acid substitutions (*11*, *13*, *20*). Earlier studies emphasized recognition of the highly homologous N-terminal region by the target organism (*16*). However, more recently, Fimland et al. (*29*) have shown that the interchange of large domains of different class IIa bacteriocins, such as pedPA-1, sakP, and curA, gives chimeric peptides whose antimicrobial specificity for particular target organisms corresponds to the C-terminal region. In a related study, it has been shown that a C-terminal fragment of pediocin (residues 20−34) specifically inhibits pedPA-1 activity. However, this short peptide is not antimicrobially active and does not significantly inhibit closely related bacteriocins, such as leuA, sakP, and curA (*30*). These results suggest that the C-terminal region is involved in receptor recognition. Interestingly, large fragments of type IIa bacteriocins are inactive, and in certain cases, deletion or alteration of a single amino acid near the C terminus (e.g., removal of terminal tryptophan from mesentericin Y105 or generation of F33S mutant of cbnB2) can render them completely inert (*22*). Although the above studies show that most of the amino acid residues in these peptides are essential for maximal activity, the key structural features necessary for recognition of the target receptor molecule in three-dimensional space remained elusive. Detailed knowledge of the structures of these bacteriocins and the effects of altering their geometries is essential for understanding their interaction with a protein receptor. Therefore, a primary goal of this study was to compare, under varying conditions, the three-dimensional structures and antimicrobial activity of representative class IIa bacteriocins, namely, pedPA-1, entP, sakP, curA, leuA, and cbnB2.

Certain class IIa bacteriocin like pedPA-1, diversion V41, entA contain a second C-terminal disulfide bond (*23*, *56*, *57*) in addition to the conserved N-terminal disulfide bond. This second disulfide bond generally affords enhanced potency and broader activity spectra compared to single disulfide peptides such as sakP and curA (*31*, *39*) and, when removed or reduced, drastically decreases in potency (*31*, *58*). Moreover, when a second C-terminal disulfide bond is introduced into sakP, target-cell specificity broadens and activity at higher temperatures increases (*59*). Very recently, the NMR solution structures of sakP and its mutant sakP-[N24C+44C], having an additional disulfide bond in the C-terminal region, were determined (*20*). Interestingly, the introduction of the second disulfide bond in sakP did not cause any major structural rearrangements. Thus, this second disulfide bond must function to make the conserved C-terminal domain structure more constrained and less amenable to change such as disruption of the helix.

Comparison of CD Spectra and Activity. Pure pedPA-1 readily transforms under aerobic conditions to a much less-active derivative via oxidation of methionine 31 to the corresponding sulfoxide. Therefore, a mutant of pedPA-1, ped[M31Nle], was synthesized by solid-phase peptide synthesis using orthogonal protection of four cysteine residues. Special measures were taken during the chemical oxidation of these cysteines to form the disulfide bonds with correct geometry. In particular, the formation of the second disulfide bond, which spans most of the C-terminal helical region was done in TFE/water to ensure proper folding. A comparison of secondary structural elements by CD showed that the synthetic pediocin mutant, ped[M31Nle] and native pedPA-1 are very similar as shown in Table 3. In a recent CD study, Watson et al. (*14*) reported that pedPA-1 contains 66% helix in 90% TFE (1 mM KMES buffer at pH 6). In our study, this peptide showed only 35% helix in 90% TFE (0.1% TFA at pH 2.5). This difference in overall helical content could be a consequence of the buffer, solvent, or peptide aggregation as mentioned by the authors themselves. In other solvent conditions, like 5 mM SDS, 5 mM DPC, a mixture of SDS−DPC, and membrane vesicles derived from *L. innocua*, all buffered to a pH of 6 with 1 mM KMES, the same authors found pedPA-1 with 32−38% helical structure.

In terms of antimicrobial activity, synthetic ped[M31Nle] is equally potent to native pedPA-1 (Table 2). Previous site-specific mutagenesis experiments to generate small quantities of peptides indicated that replacing Met31 by hydrophobic residues, such as Ala, Ile, or Leu, maintained the activity of

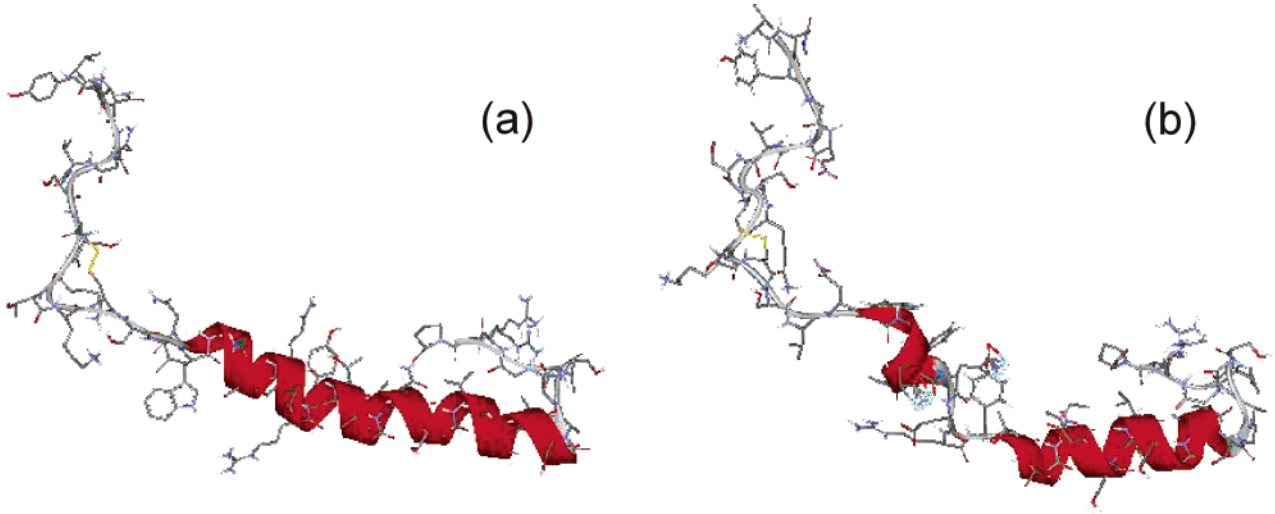

FIGURE 6: (a) NMR structure of cbnB2 in TFE at 298 K (*13*). (b) Minimized average structure over the last 1 ns of simulation in TFE for cbnB2 at 313 K.

Table 6: Comparison of the Secondary Structure of Various Class IIa Bacteriocins in TFE at Different Temperatures

bacteriocin	secondary structure determination	temp (°C)	α helix	β sheet	coil
pedPA-1	CD[a]	25	0.35	0.15	0.49
	MD	25	0.34	0.15	0.50
	MD	40	0.34	0.15	0.50
entP	MD	25	0.43	0	0.56
	MD	40	0.36	0	0.64
sakP	NMR[a,b]	25	0.31	0.10	0.59
	MD	25	0.37	0.20	0.42
	MD	40	0.30	0.18	0.51
curA	MD	25	0.41	0	0.58
	MD	40	0.32	0	0.67
leuA	NMR[a,b]	25	0.35	0.18	0.46
	MD	25	0.35	0.20	0.44
	MD	40	0.27	0.27	0.45
cbnB2	NMR[a,b]	25	0.43	0	0.56
	MD	25	0.44	0	0.55
	MD	40	0.37	0	0.62

[a] CD and NMR samples were in TFE/H_2O (9:1, v/v) containing 0.1% TFA (pH 2.5). [b] Values for leuA, cbnB2, and sakP were taken from refs *11*, *13*, and *20*, respectively.

the bacteriocin, whereas replacement by Asp was highly deleterious (*32*). This key residue falls in the amphipathic C-terminal helix region, and in oxidized pedPA-1, the alteration of the electronic and possibly steric properties of the hydrophobic suface may cause deviation from the correct spatial position necessary for receptor recognition and activity. This suggestion is further supported by the fact that pedPA-1 and ped[M31Nle] show similar activity at 25 and 37 °C, whereas the single disulfide-containing peptides such as leuA and cbnB2 that have a flexible C-terminal helical region display decreased activity at 37 °C as compared to 25 °C. Previously, Fimland et al. reported that sakP was about 10−40 times less potent at 37 °C than at 20 °C (*59*). In the same study, the authors showed that a mutant of pedPA-1, ped[C24S+C44S], wherein the C-terminal disulfide bond is removed, is less-active at elevated temperatures. However, an N24C+44C sakP mutant with an additional C-terminal disulfide bond introduced into the helical region had similar activity at 20 and 37 °C.

Effect of Temperature on Structure. TFE is a solvent that can induce defined conformations in small peptides that normally exhibit no stable secondary structure in aqueous solutions. Experimental evidence suggests that the low dielectric constant and hydrogen-bonding effects play key roles in the TFE−peptide interaction and that the resulting peptide structures are likely to approximate those in lipid environments (*18*, *19*). Hong et al. found that SDS micelles-dependent conformational transitions of melittin, a 26-residue amphiphilic peptide from honeybee venom, resemble those induced by TFE. Our earlier NMR studies show that leuA and cbnB2 adopt a well-defined tertiary structure in TFE, whereas these peptides are essentially unstructured in water or aqueous DMSO (*11*−*13*). Moreover, the structure of leuA in TFE−water closely resembles that in DPC micelles and, in the C-terminal α-helical region, is nearly superimposable in the two solvent systems. The RMSD (backbone atoms only, N, Cα, carbonyl carbon) for the superimposition of α-helical residues in leuA in DPC and TFE, leuA in DPC, and cbnB2 in TFE of 0.44 and 1.26 Å, respectively, indicates that the α-helix region is very similar in the two different media. More recently, Uteng et al. have shown that the overall appearance of the sakP NMR spectra in DPC and TFE is quite similar (*20*). The RMSD over the backbone atoms for the α-helical residues (18−33) in DPC and TFE for sakP is 0.75 Å. Thus, aqueous TFE was chosen as a solvent to perform CD and MD simulations of the bacteriocins studied in this paper. CD analysis of peptides with an additional C-terminal disulfide bond such as ped[M31Nle] and peptides without the C-terminal disulfide bond such as leuA and cbnB2 at different temperatures indicated that the former maintained its secondary structure at different temperatures. However, the later peptides with a flexible C-terminal region showed a decrease in the α-helical content at higher temperatures (37 °C). A closer look at the three-dimensional structures of these peptides using MD simulations further supported these results.

MD structures of pedPA-1, entP, and curA along with solution structures of leuA, cbnB2, and sakP suggest that the C-terminal region in all of these bacteriocins is structurally conserved despite extensive differences in the amino acid sequence. All peptides form an amphipathic α helix that

spans from the center toward the C terminus (15−20 residues). As shown in Figures 4, 5, and 6, the hydrophobic side of the amphipathic helix faces away from the more hydrophilic side, which in general faces the polar and charged residues from the N-terminal β sheet or the coil region. Trp33 is one of the conserved residues present in the hydrophobic face of the amphipathic helix of pedPA-1, sakP, and curA. It has been shown that the Trp33 residue of sakP can be replaced by any hydrophobic residue while maintaining full activity of the bacteriocin (*28*). MD simulations at a higher temperature (313 K) showed that peptides, such as entP, sakP, curA, and cbnB2, without the C-terminal disulfide bond, experienced some unfolding of the conserved helical region. In general, the uncoiling of the helix occurred in the middle of the helical region or toward the N-terminal side of the helix. MD simulation structures at 313 K for entP, sakP, curA, and cbnB2 are shown in parts b, d, and f of Figure 3 and Figure 5b, respectively. In contrast, the pedPA-1 structure did not change during the entire simulation trajectory at 313 K. The presence of the C-terminal disulfide bond in pedPA-1 provides its structure with less flexibility and corresponding temperature stability. These results combined with the antimicrobial activity results at 25 and 37 °C support the idea that the hydrophobic residues on this helix must directly interact with the receptor protein. All of the experiments consistently show that slight perturbation in the structure in this domain causes a decrease in the antimicrobial activity. Uteng et al. reported CD studies showing that a variant of sakP, sakP[N24C+44C], with an additional C-terminal disulfide bond, does display a marked decrease in the helical content when the temperature is raised from 12−52 °C (*20*). At very high temperatures such as 52 °C (as opposed to 37 °C), it is possible that the second disulfide bond is no longer capable of sufficiently restraining the conformation of the helical region at the C terminus.

Mechanism of Action. Recent studies support the interaction of class IIa bacteriocins acting with a specific receptor protein on the target cell (*33*−*36*). The additional domain present in the IID subunit of mannose PTS permease of the target cell has been proposed to be responsible for this specific interaction (*35*). This domain contains many hydrophobic residues, which may be present at the bacteriocin recognition surface, and could be involved in the specific interaction with the hydrophobic residues of the C-terminal amphipathic helix of the antimicrobial peptide. When all of the structural and activity studies of class IIa bacteriocins are taken into account, the following model for the mode of action of these peptides may be proposed. Initially the peptide may bind the cell surface, mediated by electrostatic interactions involving the positively charged N-terminal half and the hydrophilic side of the amphipathic helix region. This may be followed by specific interactions of the hydrophobic residues with the extracellular loop of the receptor protein. This tight binding could then initiate pore formation in the membrane and leakage of cellular contents. Alternatively, the bacteriocin−receptor binding could disrupt the normal function of the PTS, leading to disruption of its regulatory functions or possibly to nonproductive phosphate ester hydrolysis with concomitant depletion of phosphoenol pyruvate. Either mechanism could lead to bacteriostatic and bacteriocidal effects, but additional studies will be needed to decipher the details of this mechanism.

CONCLUSION

Class IIa bacteriocins form a β sheet or coil-like structure in the N-terminal domain and an α-helical structure in the C-terminal domain. We have studied the structure−activity relationship among these peptides using pedPA-1, which has an additional C-terminal disulfide bond, and peptides such as entP, sakP, curA, leuA, and cbnB2, which do not contain the C-terminal disulfide bond. A more stable M31Nle mutant of pedPA-1 was synthesized to study the importance of the α-helix content in relation to the activity of the peptide. Using CD and MD simulations, the structures of these peptides were compared at different temperatures. In this study, we have generated MD structures of four class IIa bacteriocins, pedPA-1, entP, sakP, and curA in aqueous TFE and water. The simulations show that the structures of these peptides are more stable in TFE compared to water. In aqueous TFE, they maintain a conserved amphipathic α helix in the C-terminal region and a β sheet or random coil in the N-terminal region. The C-terminal disulfide bond in pedPA-1 helps in maintaining the tertiary structure of the peptide in TFE even at higher temperatures, whereas peptides such as entP, sakP, curA, leuA, and cbnB2, without the C-terminal disulfide bond, experience significant structural perturbation in the amphipathic helix region. The hydrophobic residues of the C-terminal helical domain orient themselves on one side of the helix, thereby facilitating specific interaction with the receptor protein (probably a region of the mannose PTS subunit IID) on the target cell. These studies provide a structural basis to help elucidate the receptor-mediated recognition mechanism of action of class IIa bacteriocins. Furthermore, we found that the helical structure as well as the activity of pediocin-like peptides with the second (C-terminal) disulfide bond remained the same at 25 and 37 °C. However, for peptides without the C-terminal disulfide bond, there was a loss in the helical content as well as activity at elevated temperatures. These results suggest that the α helix is critical for activity.

ACKNOWLEDGMENT

We thank Mr. Robert Luty of Department Biochemistry, University of Alberta, for performing CD experiments. We are grateful to Dr. Karen E. Kawulka and Dr. Tara Sprules for helpful assistance and discussions. These investigations were supported by the Natural Sciences and Engineering Research Council of Canada (NSERC) and by the Canada Research Chair in Bioorganic and Medicinal Chemistry. K.K. gratefully acknowledges partial financial support from the Dean of Engineering and Office of the VP Academic, University of Alberta. L.C.A. gratefully acknowledges partial financial support from the Protein Engineering Networks of Centre of Excellence (PENCE).

SUPPORTING INFORMATION AVAILABLE

Minimized average structures of sakP (Figure S7A) and curA (Figure S7B) over the last 1 ns of simulation at 298 K in water, as well as PDB files for energy-minimized MD simulation structures of pedPA-1, entP, sakP, and curA in TFE at 298 K. This material is available free of charge via the Internet at http://pubs.acs.org.

REFERENCES

1. Axelsson, L. (1998) *Lactic Acid Bacteria: Classfication and Physiology*, Marcel Dekker Inc., New York.

2. Nikaido, H. (1995) Molecular genetics of bacterial pathogenesis—A tribute to Falkow, Stanley—Miller, V. L., Kaper, J. B., Portnoy, D. A., Isberg, R. R., *Science 267*, 547−547.
3. Ennahar, S., Sashihara, T., Sonomoto, K., and Ishizaki, A. (2000) Class IIa bacteriocins: Biosynthesis, structure, and activity, *FEMS Microbiol. Rev. 24*, 85−106.
4. Eijsink, V. G. H., Axelsson, L., Diep, D. B., Havarstein, L. S., Holo, H., and Nes, I. F. (2002) Production of class II bacteriocins by lactic acid bacteria; an example of biological warfare and communication, *Antonie van Leeuwenhoek 81*, 639−654.
5. Hastings, J. W., Sailer, M., Johnson, K., Roy, K. L., Vederas, J. C., and Stiles, M. E. (1991) Characterization of leucocin-A-Ual-187 and cloning of the bacteriocin gene from leuconostoc-gelidum, *J. Bacteriol. 173*, 7491−7500.
6. Moll, G. N., Konings, W. N., and Driessen, A. J. M. (1999) Bacteriocins: Mechanism of membrane insertion and pore formation, *Antonie van Leeuwenhoek 76*, 185−198.
7. Chikindas, M. L., Garciagarcera, M. J., Driessen, A. J. M., Ledeboer, A. M., Nissen-Meyer, J., Nes, I. F., Abee, T., Konings, W. N., and Venema, G. (1993) Pediocin PA-1, a bacteriocin from *Pediococcus acidilactici* pac1.0, forms hydrophilic pores in the cytoplasmic membrane of target cells, *Appl. Environ. Microbiol. 59*, 3577−3584.
8. Kazazic, M., Nissen-Meyer, J., and Fimland, G. (2002) Mutational analysis of the role of charged residues in target-cell binding, potency, and specificity of the pediocin-like bacteriocin sakacin P, *Microbiology 148*, 2019−2027.
9. van Belkum, M. J., and Stiles, M. E. (2000) Nonlantibiotic antibacterial peptides from lactic acid bacteria, *Nat. Prod. Rep. 17*, 323−335.
10. Nes, I. F., and Hole, H. (2000) Class II antimicrobial peptides from lactic acid bacteria, *Biopolymers 55*, 50−61.
11. Gallagher, N. L. F., Sailer, M., Niemczura, W. P., Nakashima, T. T., Stiles, M. E., and Vederas, J. C. (1997) Three-dimensional structure of leucocin A in trifluoroethanol and dodecylphosphocholine micelles: Spatial location of residues critical for biological activity in type IIa bacteriocins from lactic acid bacteria, *Biochemistry 36*, 15062−15072.
12. Sailer, M., Helms, G. L., Henkel, T., Niemczura, W. P., Stiles, M. E., and Vederas, J. C. (1993) ^{15}N-labeled and ^{13}C-labeled media from *Anabaena* sp. for universal isotopic labeling of bacteriocins—NMR resonance assignments of leucocin-A from leuconostoc-gelidum and nisin-A from *Lactococcus lactis*, *Biochemistry 32*, 310−318.
13. Wang, Y., Henz, M. E., Gallagher, N. L. F., Chai, S., Gibbs, A. C., Yan, L. Z., Stiles, M. E., Wishart, D. S., and Vederas, J. C. (1999) Solution structure of carnobacteriocin B2 and implications for structure−activity relationships among type IIa bacteriocins from lactic acid bacteria, *Biochemistry 38*, 15438−15447.
14. Watson, R. M., Woody, R. W., Lewis, R. V., Bohle, D. S., Andreotti, A. H., Ray, B., and Miller, K. W. (2001) Conformational changes in pediocin AcH upon vesicle binding and approximation of the membrane-bound structure in detergent micelles, *Biochemistry 40*, 14037−14046.
15. Papathanasopoulos, M. A., Dykes, G. A., Revol-Junelles, A. M., Delfour, A., von Holy, A., and Hastings, J. W. (1998) Sequence and structural relationships of leucocins A-, B-, and C-TA33a from *Leuconostoc mesenteroides* TA33a, *Microbiology 144*, 1343−1348.
16. Fleury, Y., Dayem, M. A., Montagne, J. J., Chaboisseau, E., LeCaer, J. P., Nicolas, P., and Delfour, A. (1996) Covalent structure, synthesis, and structure−function studies of mesentericin Y 105(37), a defensive peptide from Gram-positive bacteria *Leuconostoc mesenteroides*, *J. Biol. Chem. 271*, 14421−14429.
17. Fioroni, M., Diaz, M. D., Burger, K., and Berger, S. (2002) Solvation phenomena of a tetrapeptide in water/trifluoroethanol and water/ethanol mixtures: A diffusion NMR, intermolecular NOE, and molecular dynamics study, *J. Am. Chem. Soc. 124*, 7737−7744.
18. Hong, D. P., Hoshino, M., Kuboi, R., and Goto, Y. (1999) Clustering of fluorine-substituted alcohols as a factor responsible for their marked effects on proteins and peptides, *J. Am. Chem. Soc. 121*, 8427−8433.
19. Roccatano, D., Colombo, G., Fioroni, M., and Mark, A. E. (2002) Mechanism by which 2,2,2-trifluoroethanol/water mixtures stabilize secondary-structure formation in peptides: A molecular dynamics study, *Proc. Natl. Acad. Sci. U.S.A. 99*, 12179−12184.
20. Uteng, M., Hauge, H. H., Markwick, P. R. L., Fimland, G., Mantzilas, D., Nissen-Meyer, J., and Muhle-Goll, C. (2003) Three-dimensional structure in lipid micelles of the pediocin-like antimicrobial peptide sakacin P and a sakacin P variant that is structurally stabilized by an inserted C-terminal disulfide bridge, *Biochemistry 42*, 11417−11426.
21. Schiffer, M., and Edmundson, A. B. (1967) Use of helical wheels to represent the structures of proteins and to identify segments with helical potential, *Biophys. J. 7*, 121−135.
22. Quadri, L. E. N., Yan, L. Z., Stiles, M. E., and Vederas, J. C. (1997) Effect of amino acid substitutions on the activity of carnobacteriocin B2—Overproduction of the antimicrobial peptide, its engineered variants, and its precursor in *Escherichia coli*, *J. Biol. Chem. 272*, 3384−3388.
23. Marugg, J. D., Gonzalez, C. F., Kunka, B. S., Ledeboer, A. M., Pucci, M. J., Toonen, M. Y., Walker, S. A., Zoetmulder, L. C. M., and Vandenbergh, P. A. (1992) Cloning, expression, and nucleotide-sequence of genes involved in production of pediocin-PA-1, a Bacteriocin From *Pediococcus acidilactici* Pac1.0, *Appl. Environ. Microbiol. 58*, 2360−2367.
24. Cintas, L. M., Casaus, P., Havarstein, L., Hernandez, P. E., and Nes, I. F. (1997) Biochemical and genetic characterization of enterocin P, a novel sec-dependent bacteriocin from *Enterococcus faecium* P13 with a broad antimicrobial spectrum, *Appl. Environ. Microbiol. 63*, 4321−4330.
25. Tichaczek, P. S., Vogel, R. F., and Hammes, W. P. (1994) Cloning and sequencing of sakP encoding sakacin-P, the bacteriocin produced by *Lactobacillus sake* Lth-673, *Microbiology 140*, 361−367.
26. Quadri, L. E. N., Sailer, M., Roy, K. L., Vederas, J. C., and Stiles, M. E. (1994) Chemical and genetic characterization of bacteriocins produced by *Carnobacterium piscicola* Lv17b, *J. Biol. Chem. 269*, 12204−12211.
27. Tichaczek, P. S., Vogel, R. F., and Hammes, W. P. (1993) Cloning and sequencing of curA encoding curvacin-A, the bacteriocin produced by *Lactobacillus curvatus* Lth1174, *Arch. Microbiol. 160*, 279−283.
28. Fimland, G., Eijsink, V. G. H., and Nissen-Meyer, J. (2002) Mutational analysis of the role of tryptophan residues in an antimicrobial peptide, *Biochemistry 41*, 9508−9515.
29. Fimland, G., Blingsmo, O. R., Sletten, K., Jung, G., Nes, I. F., and Nissen-Meyer, J. (1996) New biologically active hybrid bacteriocins constructed by combining regions from various pediocin-like bacteriocins: The C-terminal region is important for determining specificity, *Appl. Environ. Microbiol. 62*, 3313−3318.
30. Fimland, G., Jack, R., Jung, G., Nes, I. F., and Nissen-Meyer, J. (1998) The bactericidal activity of pediocin PA-1 is specifically inhibited by a 15-mer fragment that spans the bacteriocin from the center toward the C terminus, *Appl. Environ. Microbiol. 64*, 5057−5060.
31. Miller, K. W., Schamber, R., Osmanagaoglu, O., and Ray, B. (1998) Isolation and characterization of pediocin AcH chimeric protein mutants with altered bactericidal activity, *Appl. Environ. Microbiol. 64*, 1997−2005.
32. Johnsen, L., Fimland, G., Eijsink, V., and Nissen-Meyer, J. (2000) Engineering increased stability in the antimicrobial peptide pediocin PA-1, *Appl. Environ. Microbiol. 66*, 4798−4802.
33. Ramnath, M., Beukes, M., Tamura, K., and Hastings, J. W. (2000) Absence of a putative mannose-specific phosphotransferase system enzyme IIAB component in a leucocin-A-resistant strain of Listeria monocytogenes, as shown by two-dimensional sodium dodecyl sulfate−polyacrylamide gel electrophoresis, *Appl. Environ. Microbiol. 66*, 3098−3101.
34. Hechard, Y., Pelletier, C., Cenatiempo, Y., and Frere, J. (2001) Analysis of σ(54)-dependent genes in *Enterococcus faecalis*: A mannose PTS permease (EIIMan) is involved in sensitivity to a bacteriocin, mesentericin Y105, *Microbiology 147*, 1575−1580.
35. Dalet, K., Cenatiempo, Y., Cossart, P., and Hechard, Y. (2001) A σ(54)-dependent PTS permease of the mannose family is responsible for sensitivity of Listeria monocytogenes to mesentericin Y105, *Microbiology 147*, 3263−3269.
36. Yan, L. Z., Gibbs, A. C., Stiles, M. E., Wishart, D. S., and Vederas, J. C. (2000) Analogues of bacteriocins: Antimicrobial specificity and interactions of leucocin A with its enantiomer, carnobacteriocin B2, and truncated derivatives, *J. Med. Chem. 43*, 4579−4581.
37. Tam, J. P. (1987) Synthesis of biologically active transforming growth factor α, *Int. J. Pept. Protein Res. 29*, 421−431.
38. Zhang, L., Goldammer, C., Henkel, B., Zuhl, F., Panhaus, G., Jung, G., and Bayer, E. (1995) in *Innovation and Perspectives in Solid-*

Phase Synthesis (Epton, R., Ed.) pp 711−716, 3rd Symposium, Mayflower Scientific, Ltd., Oxford, U.K.

39. Eijsink, V. G. H., Skeie, M., Middelhoven, P. H., Brurberg, M. B., and Nes, I. F. (1998) Comparative studies of class IIa bacteriocins of lactic acid bacteria, *Appl. Environ. Microbiol. 64*, 3275−3281.
40. Sreerama, N., and Woody, R. W. (2000) Estimation of protein secondary structure from circular dichroism spectra: Comparison of CONTIN, SELCON, and CDSSTR methods with an expanded reference set, *Anal. Biochem. 287*, 252−260.
41. Boeckmann, B., Bairoch, A., Apweiler, R., Blatter, M. C., Estreicher, A., Gasteiger, E., Martin, M. J., Michoud, K., O'Donovan, C., Phan, I., Pilbout, S., and Schneider, M. (2003) The SWISS−PROT protein knowledgebase and its supplement TrEMBL in 2003, *Nucleic Acids Res. 31*, 365−370.
42. Berman, H. M., Battistuz, T., Bhat, T. N., Bluhm, W. F., Bourne, P. E., Burkhardt, K., Iype, L., Jain, S., Fagan, P., Marvin, J., Padilla, D., Ravichandran, V., Schneider, B., Thanki, N., Weissig, H., Westbrook, J. D., and Zardecki, C. (2002) The Protein Data Bank, *Acta Crystallogr., Sect. D 58*, 899−907.
43. Pearson, W. R. (1990) Rapid and Sensitive Sequence Comparison With Fastp and Fasta, *Methods Enzymol. 183*, 63−98.
44. Altschul, S. F., Gish, W., Miller, W., Myers, E. W., and Lipman, D. J. (1990) Basic local alignment search tool, *J. Mol. Biol. 215*, 403−410.
45. Guex, N., and Peitsch, M. C. (1997) SWISS-MODEL and the Swiss-PdbViewer: An environment for comparative protein modeling, *Electrophoresis 18*, 2714−2723.
46. Spoel, D. V., van Buuren, A. R., Apol, E., Meulenhoff, P. J., Tieleman, D. P., Sijbers, A. L. T. M., Hess, B., Feenstra, K. A., Lindahl, E., van Drunen, R., and Berendsen, H. J. C. (2002) *Gromacs User Manual Version 3.1.1*, Nijenborgh4, 9747 AG Groningen, The Netherlands, www.gromacs.org.
47. Gropp, W., Lusk, E., and Thakur, R. (1999) *Using MPI-2: Advanced Features of the Message-Passing Intertace*, MIT Press, Boston, MA.
48. Fioroni, M., Burger, K., Mark, A. E., and Roccatano, D. (2000) A new 2,2,2-trifluroethanol model for molecular dynamics simulations, *J. Phys. Chem. B 104*, 12347−12354.
49. Berweger, C. D., van Gunsteren, W. F., and Mullerplathe, F. (1995) Force-field parametrization by weak-coupling-reengineering SPC water, *Chem. Phys. Lett. 232*, 429−436.
50. Berendsen, C. D., Postma, J. P. M., van Gunsteren, W. F., DiNola, A., and Haak, J. R. (1984) Molecular dynamics with coupling to an external bath, *J. Chem. Phys. 81*, 3684−3690.
51. Hess, B., Bekker, H., Berendsen, H. J. C., and Fraaije, J. (1997) LINCS: A linear constraint solver for molecular simulations, *J. Comput. Chem. 18*, 1463−1472.
52. Wishart, D. S., Willard, L., and Sykes, B. D. (1995) *VADAR 1.1* in ftp://redpoll.pharmacy.ualberta.ca, University of Alberta, Edmonton, Canada.
53. *MSI* (1998) WebLab ViewerLite version 3.2 in Molecular Simulations Inc., U.K., http://molsim.vei.co.uk/weblab/.
54. Nissen-Meyer, J., and Nes, I. F. (1997) Ribosomally synthesized antimicrobial peptides: Their function, structure, biogenesis, and mechanism of action, *Arch. Microbiol. 167*, 67−77.
55. Hechard, Y., and Sahl, H. G. (2002) Mode of action of modified and unmodified bacteriocins from Gram-positive bacteria, *Biochimie 84*, 545−557.
56. Metivier, A., Pilet, M. F., Dousset, X., Sorokine, O., Anglade, P., Zagorec, M., Piard, J. C., Marion, D., Cenatiempo, Y., and Fremaux, C. (1998) Divercin V41, a new bacteriocin with two disulphide bonds produced by *Carnobacterium divergens* V41: Primary structure and genomic organization, *Microbiology 144*, 2837−2844.
57. Aymerich, T., Holo, H., Havarstein, L. S., Hugas, M., Garriga, M., and Nes, I. F. (1996) Biochemical and genetic characterization of enterocin A from *Enterococcus faecium*, a new antilisterial bacteriocin in the pediocin family of bacteriocins, *Appl. Environ. Microbiol. 62*, 1676−1682.
58. Ray, B., Schamber, R., and Miller, K. W. (1999) The pediocin AcH precursor is biologically active, *Appl. Environ. Microbiol. 65*, 2281−2286.
59. Fimland, G., Johnsen, L., Axelsson, L., Brurberg, M. B., Nes, I. F., Eijsink, V. G. H., and Nissen-Meyer, J. (2000) A C-terminal disulfide bridge in pediocin-like bacteriocins renders bacteriocin activity less temperature dependent and is a major determinant of the antimicrobial spectrum, *J. Bacteriol. 182*, 2643−2648.

BI036018E